韓國鑛物學會誌 第 4 卷 第 2 號(1991)
J. Miner. Soc. Korea, 4, 129－140(1991)

Mineralogy and Genesis of Hydrothermal Deposits in the Southeastern Part of Korean Peninsula: (2) Bobae Sericite Deposits

우리나라 동남부 지역의 열수광상에 대한 광물학적 및 광상학적 연구 : (2) 보배 견운모 광상

Soo Jin Kim (김수진)* · Chang Oh Choo(추창오)*
Hee-In Park(박희인)* · Jin Hwan Noh(노진환)**

*Department of Geological Sciences, Seoul National University, Seoul 151-742, Korea
(서울대학교 지질과학과)
**Department of Geology, Kangwon National University, Chuncheon 200-701, Korea
(강원대학교 지질학과)

ABSTRACT: Two illite polytypes, $2M_1$ and $1M_d$, have been identified from the sericite deposits of the Bobae mine, Kimhae, Kyungsangnam-do. Each polytype has characteristic grain size, chemical composition, and occurrence. $2M_1$ illite occurs predominantly in the sericitic alteration zone, while $1M_d$ illite occurs predominantly in the propylitic alteration zone, implying that the former was formed in the higher temperature than the latter. Illites can be subdivided into two types based on their crystal sizes; (1) the ㎛-sized illite which is below 0.01㎜(100㎛) in size and consists of $2M_1$ and $1M_d$ type, (2) the mm-sized illite which is above 0.01㎜ in size and consists only of $2M_1$ type. Especially illite below 1㎛ is premominantly of $1M_d$ type. Therefore, it seems likely that illite crystal size is to some extent related to the polytype. XRD data show that there is no interstratified layer in illites regardless of the crystal size and polytype.

Activity of muscovite component of the ㎛-sized illite is 0.843 while that of the mm-sized illite is 0.790. However, the latter is more similar to muscovite in crystal structure than the former is. The mm-sized illite has less Al and more K than the ㎛-sized illite. In both illites, Si contents show a positive relation to octahedral Mg. Fluid inclusion study and mineral association show that the formation temperature of illite is 270-330℃. The major chemical processes leading to the formation of sericitic deposit as well as the alteration zones are the leaching of SiO_2 from the country rock and the addition of Al_2O_3 and K_2O into the sericitic ores.

요약 : 경상남도 김해지역의 보배 견운모광상에는 두 종류의 일라이트 다형, 즉 $2M_1$과 $1M_d$로 산출된다. 이들은 입자의 크기, 화학조성 및 산출상태가 서로 다른 양상을 보인다. 2M일라이트는 견운모변질대에서 우세하게 나타나는 반면, $1M_d$일라이트는 주로 프로필리틱 변질대에서 우세하게 나타난다. 이는 $2M_1$일라이트가 $1M_d$일라이트보다 고온에서 형성되었음을 지시한다. 일라이트는 입자의 크기에 따라 마이크론 일라이트와 밀리미터 일라이크로 구분되는데 마이크론 일라이트는 100㎛ 이하의 크기를 가지며 이는 $2M_1$과 $1M_d$로 구성되어 있다. 반면 밀리미터 일라이트는 0.01㎜ 이상의 크기를 가지며 이는 전부 $2M_1$일라이트로만 되어 있다. 일라이트 결정의 크기는 어느 정도 다형과 관련이 있음을 보여준다. XRD분석에 따르면 다형과 관계없이 모든 일라이트는 혼합층상구조를 가지지 않음을 보여 준다.

마이크론 일라이트의 백운모 성분의 활동도는 0.843이고, 밀리미터 일라이트의 경우는 이 값이 0.790이므로 전자가 백운모성분의 활동도는 더 높다. 그렇지만 구조적인 특징에서는 밀리미터 일라이트가 백운모에 더 가깝다. 밀리미터 일라이트는 마이크론 일라이트보다 Al이 적은 반면 K는 더 많다. 양자의 경우 Si의 함량은 Mg의 함량과 비례하여 증가하는 경향을 보인다. 유체포유물과 광물조합을 근거로 추정된 견운모광상의 형성온도는 270-330℃범위이다. 견운모광상과 변질대를 형성시킨 주요한 화학적 작용은 모암으로부터 광체로 가면서 SiO_2의 용탈과 Al_2O_3와 K_2O의 공급이다.

INTRODUCTION

The term *sericite* often used in economic geology or petrology refers to fine-grained micaceous minerals such as illite, phengite and mixed-layered illite/smectite. There has been much ambiguities in the nomenclature of such fine-grained micas because of complexity in chemical compositions forming solid solution relationships. Phengite, by definition, is composed of two end-members, that is, muscovite and celadonite, whereas illite has two end-members, that is, muscovite and pyrophyllite. Most natural illitic materials, however, appear to contain multi-phase components such as muscovite, celadonite, pyrophyllite, and paragonite (Aagaard and Helgeson, 1983). The term *illite* used here, as recommended by Srodon and Eberl (1984), denotes non-expandable, dioctahedral, fine-grained white mica with less K than muscovite.

Hydrothermal illite in the geothermal system has been studied extensively because it can be used as a direct evidence for thermodynamic characteristics of mineral formation and reaction between fluids and country rock (Lonker and Fitz Gerald, 1990; Bishop and Bird, 1987). Alternatively, hydrothermal illite ocurring near the fault fracture zones with high permeabillity is also important because it may reflect alteration process related to hydrothermal fluids. It is generally recognized that hydrothermal illite shows transformation from $1M_d$ to $2M_1$ type to be stable with increasing temperatures (Srodon and Eberl, 1984; Velde, 1985).

The sericite deposit in the Bobae mine has been formed by hydrothermal alteration of volcanic rocks by intrusion of granodiorite. The mine produces about 36,000 tons of crude ores a year.

The purposes of the study is to investigate the mineralogical characters of hydrothermal illite and the formation process of the sericite deposit.

METHODS OF STUDY

Pure monomineral samples were prepared by handpicking under stereomicroscope and then by centrifusing powdered samples in distilled water. X-ray diffraction analysis was primarily carried out on both random and preferred oriented samples for mineral identification. Heating experiment and etylene glycol saturation treatment were also performed on the oriented samples.

Unit cell parameters of pure monomineralic samples were calculated using the LSUC program. Automatated X-ray diffractometer, Rigaku Model Rad-3C with Cu target and Kα radiation, was used for X-ray analysis.

Chemical analyses were performed using an electron microprobe, JEOL JAX-733. Polished thin sections were analyzed at 15kV with beam current of 10mA and beam diameter of 10μm. XRF analyses was performed on bulk rock samples.

Textural relations were studied using a polarizing microscope and a scanning electron microscope (SEM). Powdered samples were observed using a JEOL JEM 200CX at 200kV. Fluid inclusion was studied on double-polished sections using USGS type Gas Flow Freezing and Heating System.

RESULTS

Geology of Ore Deposits

Rocks near the Bobae mine consists mainly of the Late Cretaceous rhyodacitic tuff belonging to the Yucheon group, and the Early Tertiary granodiorite (Fig. 1). Rhyodacitic tuff is widely distributed in the northern part of the Bobae mine area, while granodiorite intruded the rhyodacitic tuff in the southern part of the area.

Rhyodacitic tuff is generally grey and/or greenish grey, but it is unsually greyish white in some area due to hydrothermal alteration. Tuff breccia is locally found in tuff. Rhyodacitic tuff often shows welding structure in which flattened glassy clasts called fiamme exist (Fig. 2-A). According to the classification by Schmid(1981), rhyodacitic tuff is classified into crystal tuff, which consists chiefly of crystal grains with subordinate vitric and lithic fragments. It is generally agreed that crystal tuff is produced by both magmatic and phreatomagmatic eruptions (Cas and Wright, 1987). Tuff shows the spherulitic texture due to devitrification. Flow structures are commonly observed. Most crystal fragments are quartz, K-feldspar and albitic plagioclase, whereas the matrix is composed of glass and fine-

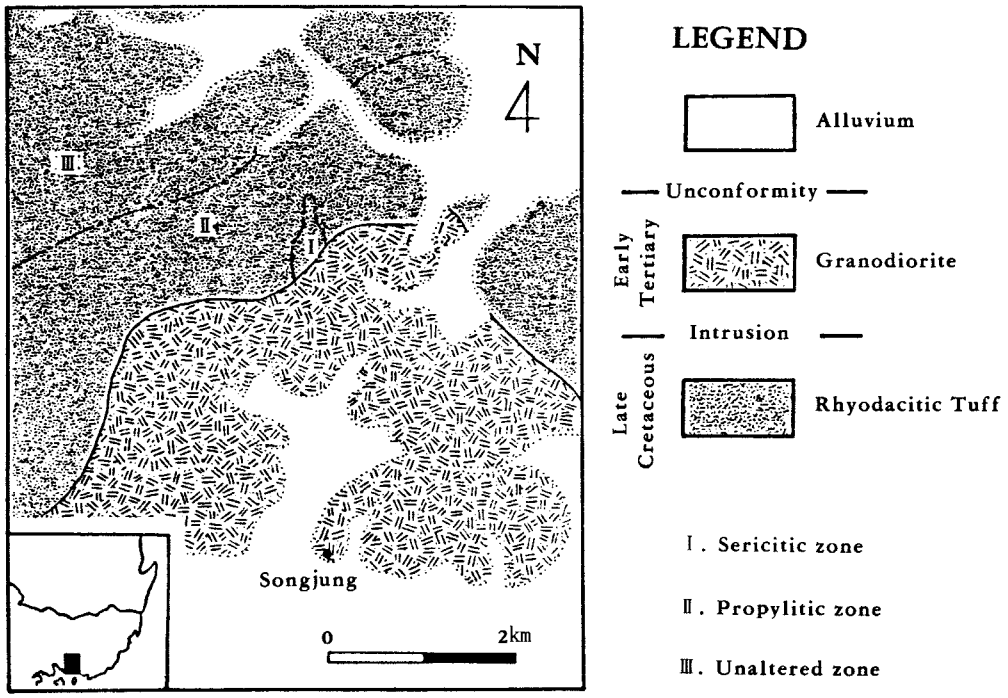

Fig. 1. Geological map around the Bobae mine.

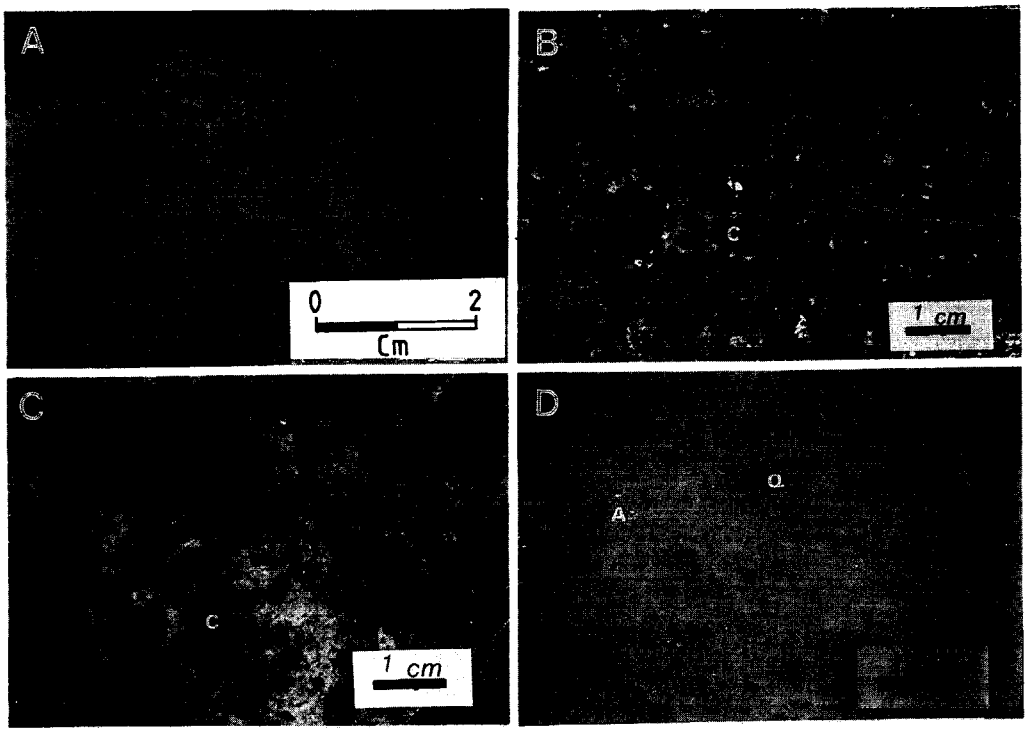

Fig. 2. Photographs of handspecimens showing various textures.
(A) Welded tuff showing the fiamme structure in the propylitic zone. (B), (C) Altered rock samples in the propylitic zone. (D) Sericite ore in the sericitic zone. Symbols are as follows: A=Andalusite; C=Chlorite; Q=Quartz

grained plagioclase. Quartz crystals show euhedral to anhedral forms. The resorption embayments are observed in some quartz and feldspar grains.

Sericite deposit of the Bobae mine is found as a massive body in rhyodacitic tuff. It is apparent that the country rock has been changed to the sericitic ores by the hydrothermal alteration that is presumable related to intrusion of granodiorite. The size of the ore body inferred from field study is roughly 250×800m. The sericitic ore body has the form of a long ellipse in NS direction.

Wall-Rock Alteration Zones

The country rocks around the sericite ore body was altered extensively by hydrothermal solution. It seems that the wall-rock alteration took place more or less irregularly. Therfore, it is difficult to define precisely the boundaries of alteration zones. The degree of hydrothermal alteration decreases gradually from the ore body toward the country rocks.

Two alteration zones are recognized based on mineral assemblages. They are sericitic and propylitic zones. The boundary between the pyropylitic zone and unaltered country rocks is gradational.

Propylitic zone: The rocks of this zone is usually greenish grey and consists of chlorite, quartz, clinozoicite, illite, pyrite, feldspars and amphibole. Illite is occasionally associated with chlorite and albite. Chlorite is common and occurs as open-space fillings, and it replaces amphibole in places (Fig. 2-B). Minor pyrite is widely disseminated within the matrix of tuff. Albite crystals whose composition is in the range of An_{4-7} Ab_{93-96} are partly alterd to micron-size illitic minerals (Fig. 3-A). Clinozoicite replaces amphibole and plagioclase, and it also occurs in veinlets. The width of the propylitic zone is wider than 1.5㎞.

Sericitic zone: Illite is the major constituent mineral of this zone (Fig. 3 and Fig. 4). Minor amounts of quartz, albite, pyrite, andalusite, pyrophyllite, apatite, and tourmaline are commonly associated. Main sericite ores are found in the middle of this zone. The zone exhibits various different colors and textures in accordance with mineral assemblages. The distribution of colors and textures of ores is so irregular at small scale that each unit of characteristic ores cannot be shown on the map. The rocks of the sericitic zone can be subdivided into three subzones according to mineral assemblages;(1) illite-andalusite subzone, (2) illite-pyrophyllite subzone, and (3) illite-albite subzone.

The illite-andalusite subzone is characterized by greenish white and pink color. Especially the greenish white part of ore consists entirely of illite. Well-crystallized illite with the size of 0.5-1.0 ㎜ are occasionally associated with pink andalusite whose crystal shape can not be recognizable under the naked-eye. The illite-pyrophyllite subzone is brownish grey and consists mainly of illite, quartz and pyrophyllite. The illite-albite subzone is white or light grey in color and consists of illite and albite. Albite occurs mainly as veinlets with the width of 5-20㎝ cutting the main ore body in random directions.

Illite occurs in two different textural types. They are relatively coarse-grained illite (called the mm-sized illite in the following) and relatively fine-grained illite (called the ㎛-sized illite in the following). The former is 0.01-0.1㎜ in size, whereas the latter is a few ㎛ in size (Fig. 3). Both types of illites occur as compact massive aggregates independently or as a mixture of both. In the mixture of both illites, their contact boundary is sharp and/or gradational. Illite aggregates are usually surrounded by fine-grained quartz aggregates in the quartz-rich rocks (Fig. 3-D).

Polytypes and Crystallinity of Illite

Two illite polytypes were identified by X-ray diffraction. The mm-sized illite (above 0.01㎜) consists of $2M_1$ polytype, whereas the micronsized illite consists of $2M_1$ and $1M_d$ types. The micron-sized illite below 1㎛ is composed mainly of $1M_d$ type with trace $2M_1$. But it is impossible to distinguish $2M_1$ and $1M_d$ individually because they are in the fine mixture. Lonker and Fitz Gerald (1990) described that there is no distict difference in morphology in transformation of $1M_d$ type to $2M_1$ type. The present study shows that the structure of illite has a tendency to change with crystallinity.

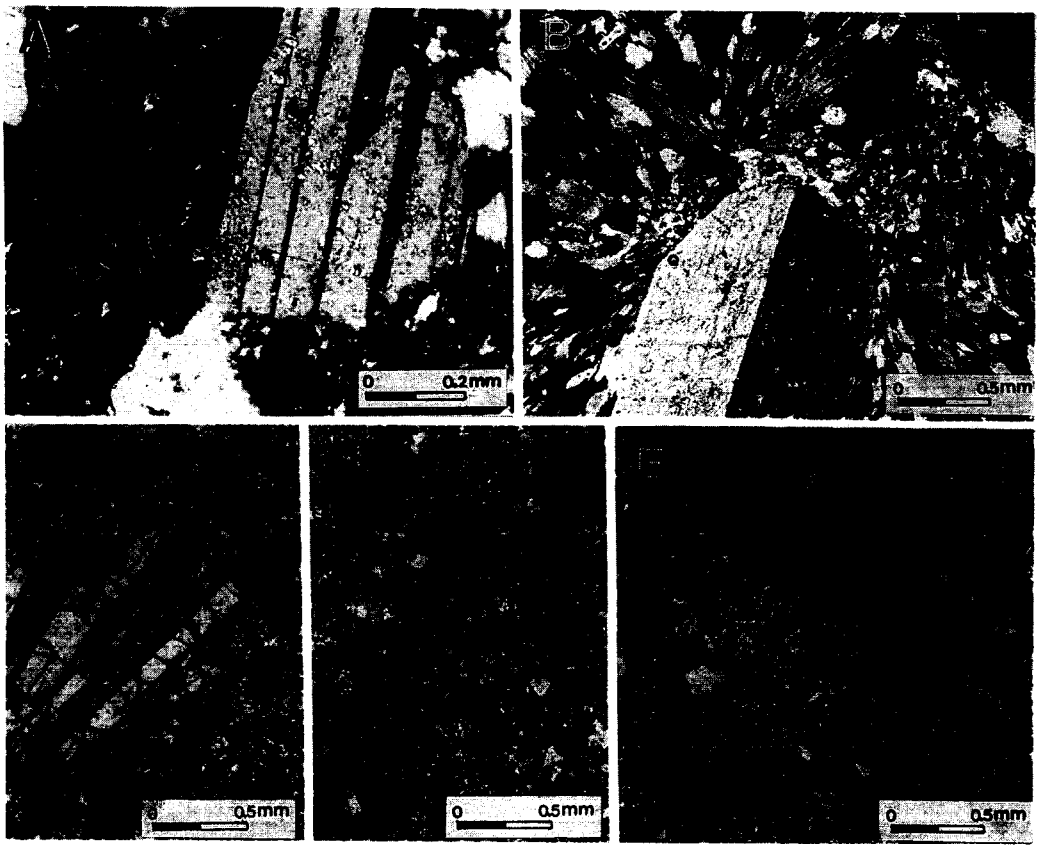

Fig. 3. Photomicrographs of typical minerals in the alteration zones. (A) Plagioclase and sericitic mineral. (B) K-feldspar (center) and quartz. (C) Andalusite (center) and illitic minerals. (D) Fine-grained quartz surrounds illitic minerals. (E) The mm-sized and ㎛-sized illites. (A) and (B) are in the propylitic zone, (C), (D) and (E) in the sericitic zone.

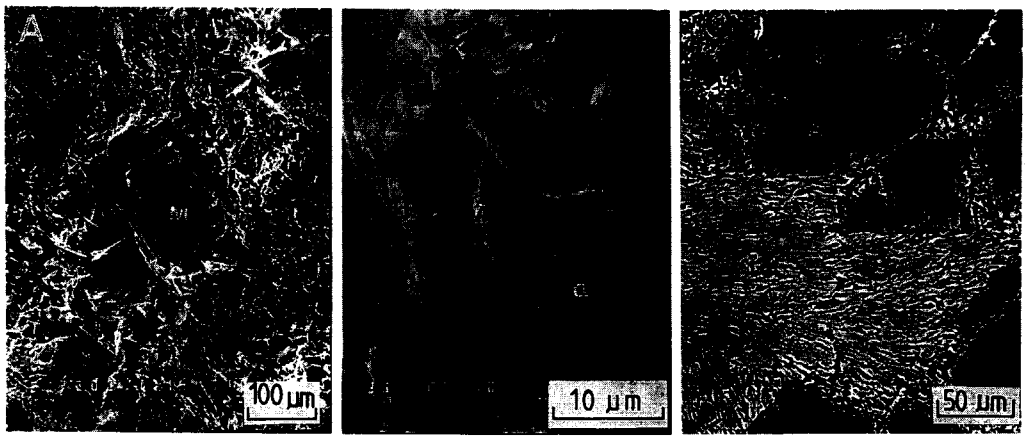

Fig. 4. SEM photographs of illites in the sericitic zone.
(A) A large muscovite in the matrix of fine-grained illite. (B) Illite flakes associated with andalusite and quartz. (C) Backscattered-electron image showing andalusite (dark grey) and illite (light grey). Symbols are as follows: A=Andalusite; I=Illite; M=Muscovite; Q=Quartz.

Table 1. Polytype proportion of illite in the alteration zones from the Bobae mine (by XRD).

	1M	$2M_1$	Sample No.
Propylitic	70%	30%	C1-3
zone	48	52	C20-8
	57	43	C2-27
	62	38	C2-95
	46	54	C2-96
Sericitic	5>	>95	B7-33
zone	5>	>95	B35
	5>	>95	B36

Table 2. Characteristics of the basal spacing of illite.

Sample	d(001)	E.G.(001)	*Ir	**K.I.
J-3	10.179	10.297	1.197	0.21
J-4	10.109	10.297	1.045	0.22
J-11	10.120	10.297	1.166	0.20
K-8	10.097	10.097	1.166	0.21
B7-22	10.120	10.097	1.022	0.26
B7-32	10.202	10.120	1.025	0.55
B7-33	10.029	10.086	1.300	0.25
B8-3	10.120	10.107	1.246	0.28
B8-5	10.086	10.086	1.116	0.45
B-36	10.120	10.202	1.127	0.21
C3-88	10.086	10.109	1.026	0.25
Mean	10.111 Å	10.161 Å	1.042	0.28

*$Ir = I(001)_{air} \times (003)_{EG} / I(001)_{EG} \times (003)_{air}$ **K.I=Kubler Index

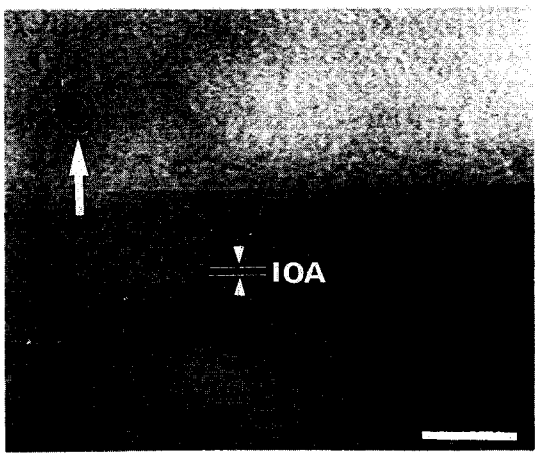

Fig. 5. TEM image of lattice fringes shows regular stacking of layers of illite. Scale bar at the bottom is 100Å long.

The ratio of $2M_1$ to 1M types in illite which were calculated following the method of Maxwell and Hower (1967) indicate that the proportion of $2M_1$ type as well as crystallinity increases from the propylitic zone toward the sericitic zone (Table 1). Illite in the high-grade sericite ores is exclusively of $2M_1$ type.

Saturation with ethylene glycol on oriented sample does not cause increase in basal spacing of illite, indicating that there is no interstratified layers in illite. Such result is also evidenced by Intensity Ratios and Kubler Index (Table 2) and by observation of lattice fringe image by TEM (Fig. 5). The refined unit cell parameters of the $2M_1$ illite from the sericitic zone are calculated to be a= 5.179Å, b=9.006Å, c=20.059Å and β=95.76°. The d(001) value is much similar to that of illite defined by Srodon and Eberl (1984). Hunziker et al. (1986) show that the value of the b-parameter increases with increasing of illite crystallinity and that illite is transformed to muscovite with increasing degree of alteration or grade of diagenesis. The b-parameter having 9.006Å of illites in this study is close to the b-parameter of illites transforming to muscovite reported by them.

It is difficult to define the difference between the structures of $2M_1$ illite and muscovite, because both minerals show nearly similar Kubler index values. This problem will be discussed in the following section.

Mineral Chemistry of Illite

It is generally acknowledged that illite is enriched in Si and deficent in K relative to muscovite. The data of chemical analyses of representative illites are given in Table 3. The net layer charge calculated, if we assume that Fe is divalent, shows little discrepancy as compared to the typical case. Therefore, all Fe in illites given here is assummed to be FeO. Table 3 shows that chemical compositions have a close relationship to the crystal sizes and occurrences. All samples analysed are plotted on the field of illite composition in the Velde's diagram of MR^3-$2R^3$-$3R^2$ (Fig. 6). Based on 11 oxygens, the mm-sized illite has generally 3.04 Si and 0.90K, whereas the μm-sized illite has commonly 3.02 Si and 0.88K.

Table 3. Electron microprobe analyses of illites from the Bobae mine.

	C20-5(A)	C20-5(B)	C20-8(A)	C20-8(B)	K13-3	B10-2	J-4
SiO_2	45.481	46.195	44.352	46.197	44.624	43.994	46.134
Al_2O_3	38.231	35.511	36.644	35.057	33.423	37.195	37.591
TiO_2	0.107	0.725	0.321	0.943	0.219	0.014	0.180
Cr_2O_3	0.050	0.093	0.000	0.307	0.000	0.063	0.000
FeO	0.298	0.798	0.849	2.284	3.908	0.143	0.496
MgO	0.000	1.162	0.165	1.011	0.886	0.016	0.000
MnO	0.007	0.142	0.000	0.000	0.034	0.010	0.143
CaO	0.071	0.029	0.071	0.032	0.007	0.000	0.045
Na_2O	0.476	0.471	0.395	0.383	0.521	0.573	0.324
K_2O	10.365	10.707	9.956	10.457	10.133	10.039	9.902
Total	95.082	95.857	92.751	96.671	93.760	92.047	94.715
	Numbers of cations on the basis of $O_{10}(OH)_2$						
Si	3.010	3.056	3.017	3.059	3.063	3.007	3.055
Al	0.990	0.944	0.984	0.951	0.938	0.994	0.946
ΣTet.	4.000	4.000	4.000	4.000	4.000	4.000	4.000
Al	1.994	1.835	1.954	1.777	1.767	2.003	1.988
Ti	0.006	0.038	0.017	0.047	0.012	0.001	0.009
Cr	0.002	0.005	0.000	0.032	0.000	0.004	0.000
Fe	0.017	0.044	0.048	0.126	0.225	0.008	0.028
Mg	0.000	0.115	0.017	0.100	0.091	0.002	0.000
Mn	0.004	0.008	0.000	0.000	0.002	0.001	0.008
ΣOct.	2.019	2.044	2.035	2.066	2.095	2.017	2.032
Ca	0.005	0.002	0.005	0.003	0.001	0.000	0.003
Na	0.061	0.061	0.052	0.049	0.079	0.076	0.042
K	0.876	0.904	0.864	0.881	0.887	0.876	0.828
ΣInt.	0.942	0.967	0.921	0.932	0.957	0.952	0.873
Tet.	−0.990	−0.944	−0.984	−0.951	−0.938	−0.994	−0.946
Oct.	0.044	0.003	0.057	0.018	−0.021	−0.040	0.070
Int.	0.947	0.969	0.926	0.935	0.958	0.952	0.876
ΣCharge	0.001	0.028	−0.001	0.002	−0.001	−0.002	0.000

Note: K13-3 (Fe-rich illite) in the propylitic zone, and others in the sericitic zone. B10-2 sample in the greenish ore. (A) denotes the μm-sized illites, whereas (B) denotes the mm-sized illites.

Fig. 7 is the plotting of chemical analyses of illites on a diagram of M^+-4Si-R^{2+}. It shows that the mm-sized illites with higher octahedral divalent cation and interlayer K content are plotted on the inner part of the diagram apart from the area of the μm-sized illites. The μm-sized illites lie on the area closer to muscovite. Phengitic illite (sample No. K13-3 from the propylitic zone) enriched in Fe is high in tetrahedral Al (0.94) and relatively low in the content of interlayer K(0.88) (see Table 3). This phengitic illite is high in octahedral divalent cations; (Fe+Mg) is 0.32. Thus, it is plotted on the area toward phengite. Al-rich illite (sample No. B10-2) associated with andalusite has 0.99 tetrahedral Al, which is the highest value among illites studied. On the other hand, it has 0.87K in interlayer which is the lowest value in illites. The formation temperature of this sample is estimated to be highest in the present study. It seems clear that substitution of Al for Si in the

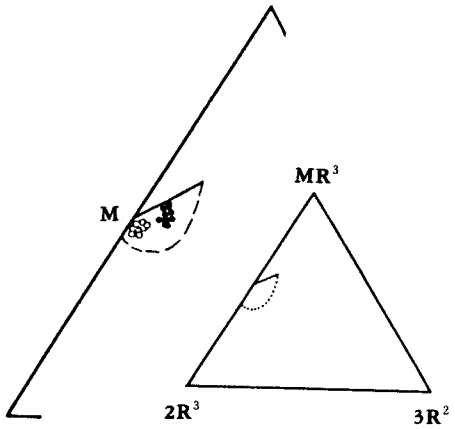

Fig. 6. Representation of illite compositions in MR^3-$2R^3$-$3R^2$coordinates near the muscovite composition(M). Solid circles are the mm-sized illite and open circles are the ㎛-sized illite, respectively.

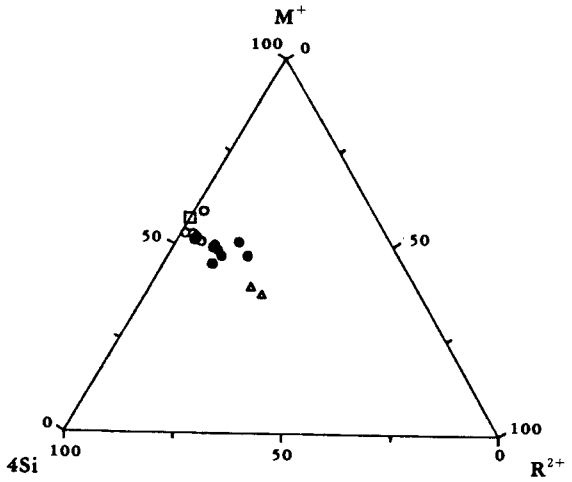

Fig. 7. Compositions of illites plotted on a M^+-4Si-R^{2+} diagram after Meunier and Velde (1989). M^+ is the layer charge, 4Si is the maximum Si content of the tetrahedral site, and R^{2+} is the total number of divalent cations in the octahedral site. A square is ideal muscovite, open circles are the ㎛-sized illite, solid circles are the mm-sized illite, and triangles are phegitic illite.

tetrahedral site depends to some extent on temperature at which illite was formed.

Although the mm-sized illite is very similar to muscovite in its K contents, the chemistry deviates considerably from that of ideal muscovite. In contrast, the composition of the ㎛-sized illite approaches to that of ideal muscovite in chemical compositon. This is because even though the mm-size illite has high K it also has relatively high Fe and Mg. Thus it is slight different from ideal muscovite. The chemical composition shows that divalent octahedral cations such as Fe and Mg also play an important role in the total layer charge. Although the mm-sized illite has less Al in the tetrahedral site than the ㎛-sized illite, the former has more K in interlayer due to higher contents of octahedral Fe and Mg which slightly contributed to total layer charge. Such result is not commonly found in the literature. Substitution of Al for Si is still largely responsible for the net layer charge deficiency in illite.

Si contents increase with increasing octahedral Mg as shown in Fig. 8. This implies that less Al substitution for Si in tetrahedral sites causes the illte structure to shift from an initial dioctahedral form toward a trioctahedral one enriched in Mg. Al is most predominant cation in octahedral sites. Octahedral Al has a negative relationship to Fe and Mg. Tetrahedral Al has nearly constant values independent of mole fractions of K in the interlayer. These results also suggest that higher K contents of the mm-sized illite relative to the ㎛-sized illite is partly due to its high contents of octahedral Fe and Mg.

Based on chemical composition and structure, activity calculation was performed. Such an approach has been made by many workers (Aagaard and Helgeson, 1983; Helgeson and Aagaard, 1985; Bird and Norton, 1981; Stoessell, 1979, 1981, 1989). Aagaard and Hegeson (1983) shows that the M(1) sites are essentially vacant in dioctahedral micas while the M(2) sites are homological and completely filled.

Natural illite and/or muscovite are composed of muscovite, pyrophyllite, celdonite, paragonite and margarite components. The characteristics of solid solution components are dependent on atoms occupying specific sites. Illite is considered here as having ideal mixing of atoms on equivalent crystallographic sites of the solid solution. The ideal mixing of atoms only refers to random mixing of atoms for which the inter-

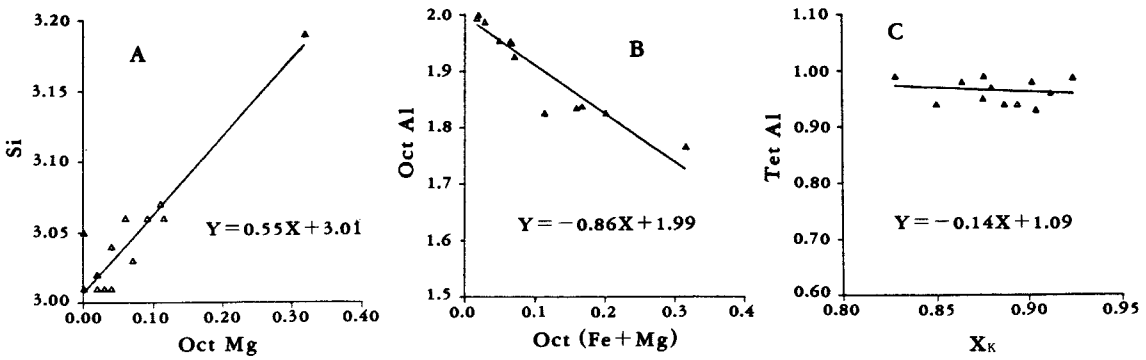

Fig. 8. Chemical relationships among various cations in illite.
(A) Si increases with increasing octahedral Mg. (B) Octahedral Al is in a negative relationshiop to Fe plus Mg in octahedral sites. (C) Tetrahedral Al is nearly constant with X_K (mole fraction of K in interlayer).

change energies are zero, with complete disorder. If ideal mixing of atoms occurs on all the sites in a solid solution, then activity coefficient of the j-th atoms on the s-th crystallographic sites in a solid solution, $\lambda_{j,s}$ becomes unity for all values of j (atoms) and s (crystallographic sites). Accordingly, this results in the following.

$$a = k \prod_s \prod_j (X_{j,s}\lambda_{j,s})^{\nu_{s,j}} = k \prod_s \prod_j (X_{j,s})^{\nu_{s,j}},$$

where k represents standard normalization constant for the i-th component and $\nu_{s,j}$ denotes stoichiometric numbers of the s-th crystallographic sites occupied by the j-th atoms in a solid solution. $X_{j,s}$ represents mole fraction of atoms in which subscripts are the same meaning as described above.

In the calcultion of activities of muscovite and pyrophyllite components, it is assumed that there is no interstratified layer in illites. Such an assumption is relatively consistent with the XRD and TEM data illustrated earlier. It is also assumed that pyrophyllite component is perfectly ordered and that muscovite component is completely disordered. Only Si, Al, K atoms are considered as participants controlling activities in the mineral system studied.

For pyrophyllite component, $a_{py}=(X_{v,A})(X_{Al,M(2)})^2(X_{Si,T})^4$ where v denotes vacancy. X is mole fraction of atoms and subscript stands for structural sites of atoms. For example, first bracket is mole fraction of vacancy in A-site of interlayer and second bracket is mole fraction of Al in M(2) site of octahedral sites.

For muscovite component, it follows that $a_{mus}=9.4815(X_{K,A})(X_{Al,M(2)})^2(X_{Al,T})(X_{Si,T})^3$, where 9.4815 is the normalization constant from the inverse value of $X_{Si}^3X_{Al}=(0.75)^3(0.25)$. X denotes mole fraction of atoms in the site corresponding to subscript.

The relationship between log a_{py} and log a_{mus} is nearly constant as in Fig. 9. This suggests that activities of paragonite and margarite excluded from calculation influence a little the activity of the other members. If there exisits no Na and Ca in interlayer, log a_{mus} may be in the negative relationship to log a_{py}. In general, illite here yields high values of log a_{mus} (Fig. 9-B). Activity of pyrophyllite is in negative relationship to mole fraction of K in interlayer. In general, activity of muscovite is related to mole fraction of K and Al.

Wall-Rock Alteration Process

Chemical and mineralogical variations between the sericitic alteration and the propylitic alteration zones were studied in order to know chemical processes controlling the hydrthermal alteration of rhyodacitic tuff. Comparison of chemical compositions of alteration zones is illustrated in Fig. 10. The sericitic zone has high content of potassium in the initially K-poor volcanic rock. SiO_2 decreases with increasing K_2O and Al_2O_3 toward the sericitic zone (symbol d) from

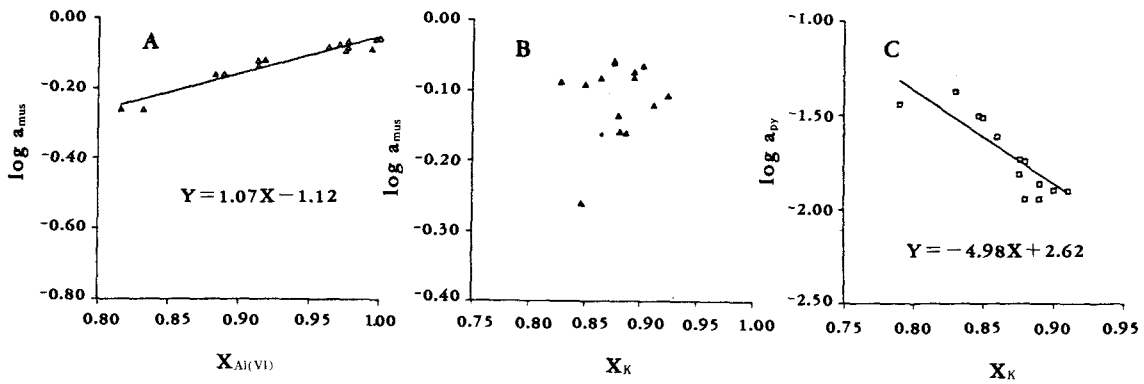

Fig. 9. Relationships between activities and mole fractions of cations.
(A) Octahedral Al is in a linear relationship to activities of muscovite component in illite. (B) Illite has generally high values of X_K and activity of muscovite component. (C) Activity of pyrophyllite component decreases with increasing X_K (mole fraction of K in interlayer).

the country rock (symbol a). Fe_2O_3 and MgO slightly increase after an abrupt drop in abundance near the boundary (symbol b) between the country rock and the propylitic zone. The high contents of Al_2O_3 and K_2O of the sericitic zone is largely due to the formation of illite. Considering this result, it is likely that the rhyodacitic tuff was subject to replacement of glass matrix and plagioclase by illite and chlorite. Al increases toward the sericitic zone.

The chemical variation shows that the main alteration processes leading to the formation of the sericite deposit and alteration zones are leaching of SiO_2 from the country rock, and addition of Al_2O_3 and K_2O into the sericitic zone.

DISCUSSION

Geological features of the Bobae sericite deposit indicate that the sericite ore was formed through the alteration process of acidic country rocks by hydrothermal fluids which was supplied from granodiorite intrusion. Temperature is an important factor controlling the formation condi-

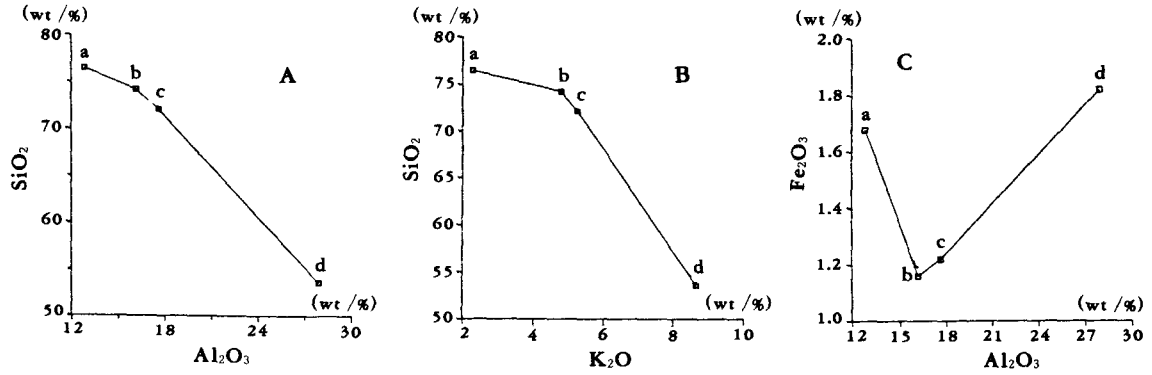

Fig. 10. Variations in chemical compositions of bulk specimens according to alteration zones (a:fresh country rock, b:propylitc zone, c:white-colored ore in the sericite zone, d:high-grade ore with green color in the sericitic zone). (A) SiO_2 decreases with increasing Al_2O_3 from the country rock toward the sericitic zone. (B) SiO_2 decreases with increasing K_2O in the same manner. (C) Fe_2O_3 (total Fe) increases gradually with increasing the alteration degree after an abrupt decreasing around the boundary of the propylitic zone and country rock.

tions under which clay minerals were formed. The ore-forming temperature estimated by homogenization temperature of fluid inclusions in quartz is in the range of 270-330℃. The highest temperature estimated is obtained from the sericite-andalusite ores. Temperatures estimated are also consistent with the range by mineral assemblages of illite-andalusite-pyrophyllite in the sericite alteration zone. Walther and Helgeson (1977) report that the lowest temperature of andalusite associated with pyrophyllite is around 340℃ in the system Al_2O_3-SiO_2-H_2O. Considering the characteristic mineral assemblage and homogenization temperatures of associated quartz, the temperature ranges given above may be acceptable as a formation temperature for the clay deposit.

Velde (1965) suggests that transformation of $1M_d$ to $2M_1$ takes place in the temperature range of 125-350℃ for ideal muscovite. In the sericitic zone, $2M_1$ illite is predominant while $1M_d$ illite is negligible. Only $2M_1$ type illite having well-crystallized grains is found in the greenish sericite ore whose formation temperature is higher relative to the propylitic zone consisting of predominant $1M_d$ illite. This means that $2M_1$ type is relatively stable in the sericitic zone, whereas $1M_d$ is unstable in this zone. But the relationship of transformation between polytypes is unknown in the present study. It appears that transformation of $1M_d$ to $2M_1$ type is usually controlled by temperature. Hunziker et al. (1986) report that the prograde evolution from $1M_d$ to $2M_1$ muscovite involves a continuous lattice reconstruction without rupture of the tetrahedral and octahedral bonds and changes of the hydroxyl radicals. Lonker and Fitz Gerald (1990) show that there exists little difference in interlayer contents among the polytypes.

Besides temperature, it seems clear that chemical composition is also an important factor controlling structural properties of illite. Rosenberg et al. (1990) report that the composition of end-member illites ranges between 0.8K and 0.9$K/O_{10}(OH)_2$ and that expandability of them is 0 %, with I-type ordering. Inasmuch as chemical composition and structural features of almost all illites under study exhibit 0.9$K/O_{10}(OH)_2$, no expandability and no mixed-layers, it is believed that illite is I-type ordering rather than ISII-type ordering.

Activity of muscovite component in the ㎛-sized illite is 0.843. It is higher than that of the mm-sized illite having 0.780. But the mole fraction of K is 0.984 in the former, whereas it is 0.924 in the latter. Considering the crystal size and mole fraction of K, the mm-sized illite is much analogous to muscovite as compared to the ㎛-sized illite. On the contrary, based on activities of muscovite component and chemical properties, the ㎛-sized illite approachs to ideal muscoveite.

CONCLUSIONS

Two hydrothemal alteration zones are recognized in the Bobae sericite deposit; the sericitic and propylitic zones. The sericitic zone is characterized by $2M_1$ illite and minor andalusite, pyrophyllite, and quartz, whereas the propylitic zone by chlorite, feldspars, clinozoicite, $1M_d$ illite, and pyrite. Illite occurs as two different grain size; mm-sized and ㎛-sized illites. The mm-sized illite is only of $2M_1$ type, whereas the ㎛-sized illite is $2M_1$ and $1M_d$ types. The former illite is more close to muscovite than the latter one in K mole fraction and crystal structure, whereas the latter illite is more close to muscovite than the former one in activities of muscovite component and chemical properties. Two types of illites have somewhat different chemical composition.

Formation temperatures of main ore body are estimated 270-330℃ by the fluid inclusion study and mineral assemblage. Polytype and crystal growth of $1M_d$ and $2M_1$ depend to great extent on temperatures, chemical compositions, and the degree of alteration. The major chemical processes leading to the formation of sericite deposits as well as the alteration zones are the leaching of SiO_2 from the country rock and the addition of Al_2O_3 and K_2O into the sericitic ores.

Acknowledgments: The present study was supported by the Basic Science Research Institute Porgram, Ministry of Education 1990, Project No. BSRI-91-505. We would like to express our appreciation to Dr. Kim, W. S. and Dr. Ahn, J. H. for their reviews of the manuscript.

REFERENCES

Aagaard, P., and Helgeson, H. C. (1983) Activity/composition relations among silicates and aqueous solutions: II. Chemical and thermodynamic consequences of ideal mixing of atoms on homological sites in montmorillonites, illite, and mixed-layer clays. Clays Clay Miner. 31, 207-247.

Bird, D. K., and Norton, D. L. (1981) Theoretical prediction of phase relations among aqueous solutions and minerals: Salton Sea geothermal systeem. Geochim. Cosmochim. Acta. 45, 1479-1493.

Bishop, B. P., and Bird, D. K. (1987) Variation in sericite composition from fracture zones within the Coso Hot Spring geeothermal system. Geochim. Cosmochim. Acta. 51, 1245-1256.

Cas, R. A. F., and Wright, J. V. (1987) Volcanic Successions: Modern and Ancient. London Allen and Unwin.

Helgeson, H. C., and Aagaard, P. (1985) Activity/composition relations among silicates and aqueous solutions. I. Thermodynamics of intrasite mixing and substitutional order/disorder in minerals. Am. Jour. Sci. 285, 769-844.

Hunziker, J. C., Frey, M. Clauer, N., Dallmeyer, R. D., Friedrichsen, H., Flehmig, W., and Hochstrasser, K. (1986) The evolution of illite to muscovite: Mineralogical and isotopic data from the Glarus Alps, Switzerland. Contri. Miner. Pet. 92, 157-180.

Lonker, S. W., and Fitz Gerald, J. D. (1990) Formation of coexisting 1M and 2M polytypes in illite from an active hydrothermal system. Amer. Miner. 75, 1282-1289.

Maxwell, D. T., and Hower, J. (1967) High-grade diagenesis and low-grade metamorphism of illite in the Precambrian Belt Series. Am. Miner. 52, 843-857.

Meunier, A., and Velde, B. (1989) Solid solutions in I/S mixed-layer minerals and illite. Amer. Miner. 74, 1106-1112.

Rosenberg, P. E., Kittrick, J. A., and Aja, S. U. (1990) Mixed-layer illite/smectite: A multiphase model. Amer. Miner. 75, 1182-1185.

Schmid, R. (1981) Descriptive nomenclature and classification of pyroclastic deposits and fragments: recommendations of the IUGS Subcommission on the Systematics of Igneous Rocks. Geology 9, 41-43.

Srodon, J., and Eberl, D. D. (1984) Illite: In: Bailey, S. W.(ed.), Micas. Reviews in Mineralogy vol. 13, 495-544.

Stoessell, R. K. (1979) A regular solution site-mixing model for illite. Geochim. Cosmochim. Acta. 43, 1151-1159.

Stoessell, R. K. (1981) Refinements in a site-mixing model for illite: Local electrostatic balance and the quasi-chemical approximation. Geochim. Cosmochim. Acta. 45, 1733-1741.

Stoessell, R. K. (1989) The quasi-lattice site-mixing model: The binary, symmetical case. Geochim. Comochim. Acta. 53, 1675-1680.

Velde, B. (1965) Experimental determination of muscovite polymorph stabilities. Am. Miner. 50, 436-449.

Velde, B. (1985) Clay Minerals: A Physico-Chemical Explanation of their Occurrence. Elsevier.

Walther, J. V., and Helgeson, H. C. (1977) Calculation of the thermodynamic properties of aqueous silica and the solubility of quartz and its polymorphs at high pressures and temperatures. Am. Jour. Sci. 277, 1315-1351.